

## Size effects in the structural phase transition of VO<sub>2</sub> nanoparticles

R. Lopez,\* T. E. Haynes, and L. A. Boatner

*Solid State Division, Oak Ridge National Laboratory, Oak Ridge, Tennessee 37831*

L. C. Feldman<sup>†</sup> and R. F. Haglund, Jr.

*Department of Physics and Astronomy, Vanderbilt University, Nashville, Tennessee 37235*

(Received 3 April 2002; published 11 June 2002)

We have observed size effects in the structural phase transition of submicron vanadium dioxide precipitates in silica. The VO<sub>2</sub> nanoprecipitates are produced by the stoichiometric coimplantation of vanadium and oxygen and subsequent thermal processing. The observed size dependence in the transition temperature and hysteresis loops of the semiconductor-to-metal phase transition in VO<sub>2</sub> is described in terms of heterogeneous nucleation statistics with a phenomenological approach in which the density of nucleating defects is a power function of the driving force.

DOI: 10.1103/PhysRevB.65.224113

PACS number(s): 65.80.+n, 42.65.Pc, 61.46.+w, 81.30.-t

### I. INTRODUCTION

A number of transition-metal oxides exhibit insulator- (or semiconductor-) to-metal transitions.<sup>1</sup> Among these, VO<sub>2</sub> is one of the most extensively studied examples because its phase transition occurs close to room temperature ( $T_c \sim 340$  K), and it displays a  $\sim 10^5$  decrease in resistivity as well as a large change in transparency in the infrared region—properties that are useful for a variety of applications. Above the phase transition, VO<sub>2</sub> has a tetragonal rutile structure while the low-temperature phase is monoclinic.<sup>2</sup> Characteristics of this transition include the formation of cation-cation pairs and the displacement of vanadium from the center of its interstice in the monoclinic phase—a feature characteristic of an antiferroelectric-type distortion.

Although there have been important advances in understanding the general nature of the transition,<sup>3–6</sup> the mechanism responsible for its nucleation is not well established. In fact, the actual values of the transition temperature and its sharpness,<sup>7</sup> or the lack thereof, have previously been related to variations in stoichiometry, misorientation between grains,<sup>8</sup> and other morphological faults<sup>9</sup> in VO<sub>2</sub> only in a qualitative fashion.<sup>10,11</sup> A more complete understanding of these features and the role of reduced dimensionality in altering the characteristics of the VO<sub>2</sub> phases is important to advancing our knowledge of the detailed physical basis of the VO<sub>2</sub> semiconductor-to-metal transition.

We have previously shown that ion implantation and thermal processing can be used to create an embedded layer of small particles of VO<sub>2</sub> in the near-surface region of an amorphous SiO<sub>2</sub> host.<sup>12</sup> These particles exhibited a hysteretic semiconducting-to-metallic phase transition with an anomalous large undercooling. (The VO<sub>2</sub> first-order transition exhibits a hysteresis that is on the order of 1–10 K wide in most cases, but in the case of VO<sub>2</sub> small particles embedded in SiO<sub>2</sub>, we observed hysteretic behavior with widths up to 50 K.) At the time of the work reported in Ref. 12, methods for controlling the mean size of the VO<sub>2</sub> precipitates in order to carry out investigations of the role of particle size on the semiconductor-to-metal phase transition had not been developed. Subsequently, we have developed techniques for cre-

ating VO<sub>2</sub> small particles with sizes that cover a relatively large range. In the work reported here, by using these assemblies of small VO<sub>2</sub> particles with varying mean size, we have been able to observe size-dependent effects in the characteristic features of the hysteretic phase transition. An analysis of these results reveals the heterogeneous nature of the nucleation process associated with the VO<sub>2</sub> phase transition, and we are able to model the observed size effects on this basis. Although other systems<sup>13</sup> have proved to exhibit size-dependent phase transitions, to our knowledge such phenomena have not been previously quantified in the case of a three-dimensional, size-controlled semiconductor-to-metal phase transition.

### II. MATERIALS SYNTHESIS AND CHARACTERIZATION

Small VO<sub>2</sub> particles in the nanoscale regime were produced by ion implantation<sup>14</sup> into a high-purity (Suprasil) SiO<sub>2</sub> substrate.<sup>12</sup> Vanadium and oxygen ions were implanted at room temperature in the near-surface region in a stoichiometric proportion. The implantation energies (150 keV for vanadium and 55 keV for oxygen ions) were calculated using the computer code TRIM (Ref. 15) and then selected to ensure the superposition of both species distributions at the same depth, within 200 nm from the surface. Rutherford backscattering spectroscopy was used to confirm the dose retention and placement. High-temperature annealing (1000 °C) in a flowing high-purity argon atmosphere induced the precipitation of the VO<sub>2</sub> nanocrystals whose size was controlled by varying the growth time in the furnace from 2 to 60 min. In order to obtain a strong VO<sub>2</sub> response during the characterization procedures, the implanted doses were  $1.5 \times 10^{17}$  ions/cm<sup>2</sup> for vanadium and  $3.0 \times 10^{17}$  ions/cm<sup>2</sup> for oxygen.

The first identification of the VO<sub>2</sub> precipitation was carried out by x-ray diffraction, using  $\theta$ - $2\theta$  scans at the Cu  $K\alpha$  wavelength. Figure 1 shows that in addition to the broad structure due to the amorphous SiO<sub>2</sub> substrate, a Bragg reflection at  $2\theta = 27.81^\circ$  is observed corresponding to the (011) reflection of the monoclinic phase.

The characterization of the particle size and the detection

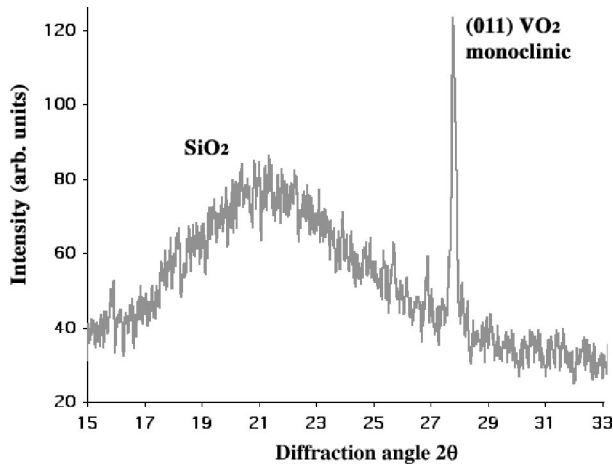


FIG. 1. X-ray  $\theta$ - $2\theta$  scans ( $\lambda = 1.5406 \text{ \AA}$ ) of fused  $\text{SiO}_2$  implanted with  $1.5 \times 10^{17} \text{ V ions/cm}^2$  at 150 keV and  $3.0 \times 10^{17} \text{ O ions/cm}^2$  at 55 keV and later annealed in flowing high-purity argon at  $1000^\circ\text{C}$  for 30 min. The characteristic diffraction line detected at  $27.81^\circ$  corresponds to the (011) plane of the low-temperature  $\text{VO}_2$  phase.

of the phase transition were performed by transmission electron microscopy (TEM) and infrared optical transmission, respectively. Figure 2 shows some representative TEM micrographs of the  $\text{VO}_2$  precipitates obtained at different annealing times along with their optical transmission at a wavelength of  $1.5 \mu\text{m}$ . Since the particles exhibit an increasing aspect ratio with increasing size, in order to simplify the analysis, the mean size values were approximated by mass weighting the radius of equivalent volume spheres. Figure 3 shows the dependence of both the particle size and the optical transmission at various temperatures on the annealing time. There is a clear correlation between the transition temperatures and the particle size: the decrease of the precipitate size produces higher transition temperatures on heating and lower temperatures on cooling, leading to increasingly wider hysteresis loops as the particles become smaller.

### III. DISCUSSION

In order to analyze the observed size dependence of the phase transition temperatures, we consider the transition in

the frame of classical nucleation theory.<sup>16</sup> The change in free energy,  $\Delta G$ , due to the formation of a spherical nucleus consists of two terms<sup>17</sup>

$$\Delta G = -\frac{4\pi}{3}R^3\Delta g_{ex} + 4\pi R^2\gamma, \quad (1)$$

where  $R$  is the radius of the nucleus and  $\Delta g_{ex}$  is the bulk free energy decrease per unit volume, which we assume is proportional to  $|T - T_c|$  with a proportionality constant determined by the entropy difference between the parent and the product phase  $0.657 \text{ MJ}/(\text{m}^3 \text{ K})$ .<sup>18</sup> Here  $\gamma$  is the surface free energy increase per unit area which can be estimated to lie in the range of  $10$ – $20 \text{ mJ/m}^2$ . This homogeneous nucleation process implies, as can be seen in Fig. 4, a barrier of  $10^{-16} \text{ J}$  per nucleation event ( $\sim 6 \times 10^2 \text{ eV}$ ), which is  $10^4 k_B T$  at temperatures where the transition occurs spontaneously. Evidently, the thermal energy is much too small for homogeneous nucleation; hence nucleation at special sites (like those observed in martensitic transformations<sup>19</sup>) must be considered. Further support for this approach comes from the direct observation of no time dependence during the transition. In fact, the growth of the product phase is extremely fast and can be completed in less than 500 fs in continuous thin films.<sup>20</sup> Accordingly, control of the transformation relies on the thermal nucleation process rather than on phase propagation as in the classical picture. Regarding the semiconductor-to-metal transition as the result of heterogeneous nucleation, its occurrence depends on the availability of a suitable nucleating defect in the sample space considered. The nature of these nucleation sites could be very diverse, ranging from simple vacancies, wall dislocations, untransformed embryonic regions, or perhaps electronic defects—given all the possible valences of vanadium. We believe these sites must be some type of extrinsic defects since the estimated densities for intrinsic defects would be too low ( $\sim 10^{11}/\text{cm}^3$ ) at the transition temperature. However, higher densities of extrinsic defects are expected to be present during the high-temperature annealing. It is possible that many of these defects persist, given the quenching process applied to the samples.

If the probability of finding a potent defect in a small volume is  $\rho dV$  and the chance to find more than one defect

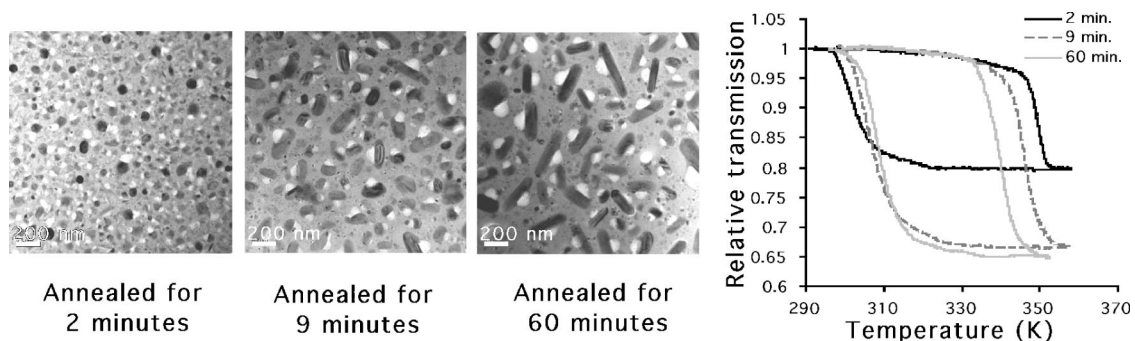


FIG. 2. Transmission electron microscopy images of  $\text{VO}_2$  precipitates in  $\text{SiO}_2$  and their optical transmission vs temperature at a  $1.5\text{-}\mu\text{m}$  wavelength for selected annealing times. Shorter annealing times produced smaller precipitates and shifted the transition temperatures to produce wider hysteresis loops. The samples were prepared by implanting  $\text{SiO}_2$  with  $1.5 \times 10^{17} \text{ V ions/cm}^2$  at 150 keV and  $3.0 \times 10^{17} \text{ O ions/cm}^2$  at 55 keV and then annealing in argon at  $1000^\circ\text{C}$ .

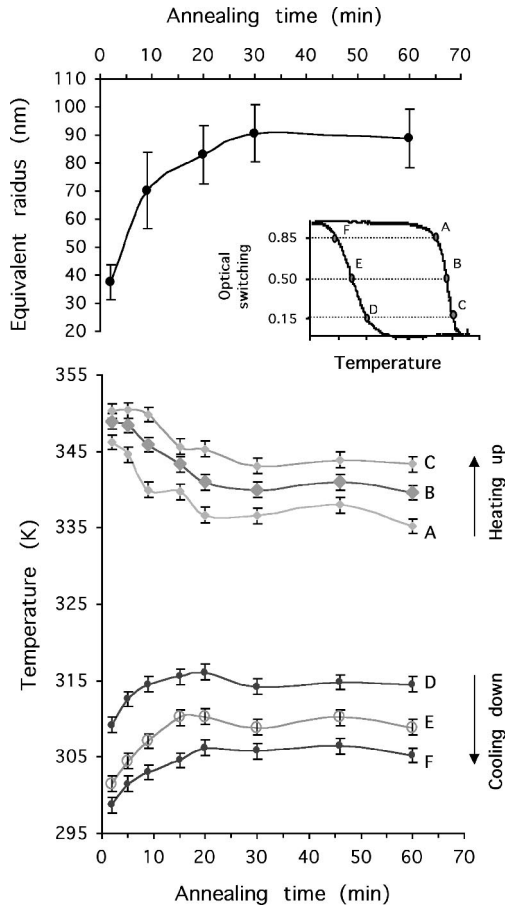


FIG. 3. (Top)  $\text{VO}_2$  precipitate size as determined by the annealing time and (bottom) the corresponding relative optical transmission or “switching” at a  $1.5\text{-}\mu\text{m}$  wavelength as a function of annealing time. The inset shows a typical hysteresis loop obtained during the thermal cycle along with the indicator points (A,B,C,D,E,F) used to quantify the optical “switching.”

is negligible, it can be shown<sup>21</sup> that the probability  $F$  that a particle of volume  $V$  contains at least one such site is<sup>22</sup>

$$F = 1 - \exp[-\rho \cdot V]. \quad (2)$$

In order to analyze the statistics of the nucleating defects at different temperatures,  $\rho$  is proposed<sup>23</sup> to be a power-law function of the driving force  $\Delta g_{ex}$ , since as the driving force increases, latent defects may become operational.<sup>24</sup> In this purely phenomenological approach,

$$\rho = C \Delta g_{ex}^y, \quad (3)$$

where  $y$  is an exponent,  $C$  a proportionality constant, and the temperature dependence is incorporated via the fact that  $\Delta g_{ex}$  is proportional to  $|T - T_c|$ , as described above. Combining Eqs. (2) and (3), we obtain the necessary function to analyze the statistics of the  $\text{VO}_2$  phase transition from the small-particle results.

Assuming that the particle size distribution is adequately parametrized by the equivalent mean radius and the relative optical transmission during the hysteresis cycle is linearly proportional to the volume fraction of  $\text{VO}_2$  that has under-

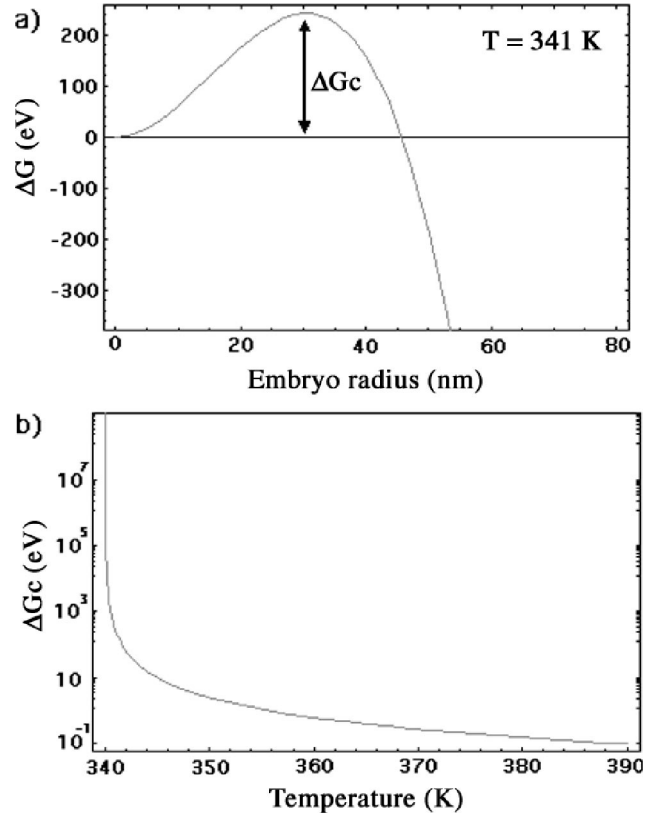


FIG. 4. (a) Free energy as a function of the nucleating embryo size during the phase transition; (b) The energy barrier as function of the temperature.

gone the phase transition, we can directly identify the probability  $F$  with that optical change. Data from the transition in both heating and cooling directions are plotted in the inset of Fig. 5, where the reference temperatures ( $T_c$ ) involved in  $\Delta g_{ex}$  were obtained by extrapolation to the point where the transition would start for bulk behavior—that is, 338 K and 325 K in the warming and cooling directions, respectively. The exponents  $y$  and the proportionality constants are obtained using least-squares fitting. The exponent for the cooling portion ( $\sim 3$ ) is larger than that on the warming side ( $\sim 2$ ) as expected from the asymmetric shear stress<sup>25</sup> present on cooling, which requires larger driving forces in order to overcome the nucleation barrier. These exponents provide an important test of any microscopic model of the defect-nucleus interaction. The phenomenological correlations found above are compared directly with the data in Fig. 5 where a temperature-modified volume is used as the abscissa. The curves correlate reasonably well with the data in the entire range of temperatures and particle sizes studied. We conclude, therefore, that the temperature and particle size dependence of the  $\text{VO}_2$  phase transition are consistent with the statistical description for a heterogeneous nucleation process.

The present results can also provide an estimate of  $\rho$  as a function of the temperature. Figure 6 shows the cumulative density of the sites for both sides of the transition. At the beginning of both transitions,  $\rho$  is around  $10^{14}$  nucleation sites/ $\text{cm}^3$ , which for particle sizes  $V \leq V_{crit}$  ( $10^{-15} \text{ cm}^3$ )

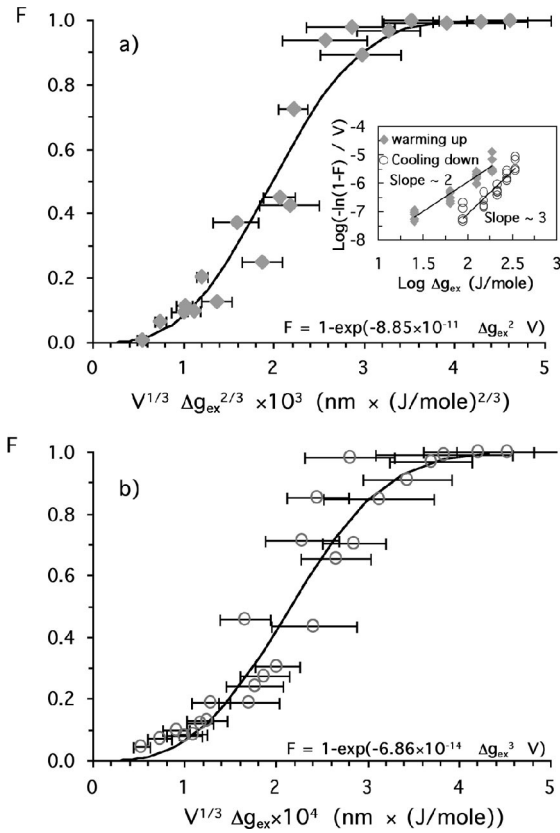


FIG. 5. The fraction of transformed particles as a function of the size and temperature; (a) on warming, (b) on cooling. Solid lines are the calculated curves using equations (2) and (3). The inset shows the linear correlations that support the proposed phenomenological expression for  $\rho$ .

means there is no potent defect present to activate the transformation and further increases in the driving force are needed to activate at least one defect. For  $V$  slightly above  $V_{crit}$ , some particles will have exactly one potent defect and the other particles will have none. In this regime, the trans-

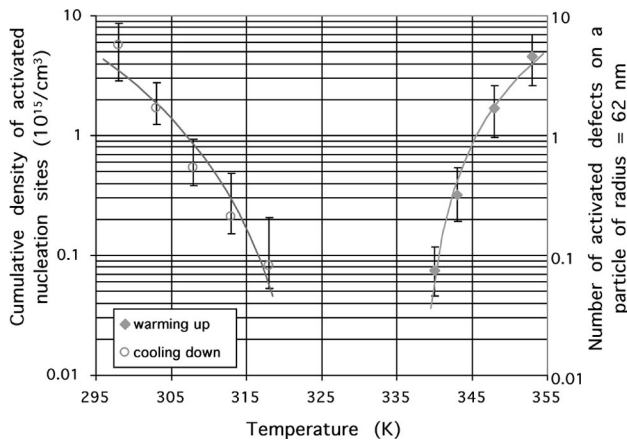


FIG. 6. Cumulative density of nucleation sites vs temperature in both directions of the semiconductor-metal transition. A particle with a 62-nm radius will have one activated site and, therefore, will start transforming near 345 or 305 K on heating or cooling, respectively.

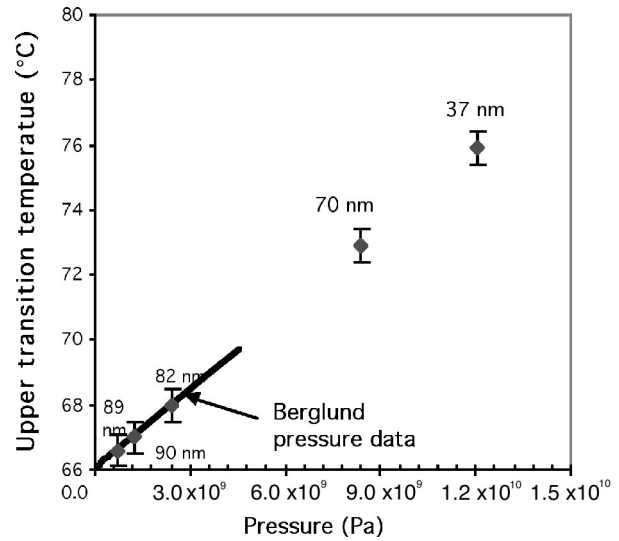


FIG. 7. Hydrostatic pressures [according to Berglund and Jayarama’s data (Ref. 26)] which would follow from the observed increases in transition temperatures. The values are far too high and, therefore, unlikely to be responsible for the observed effect.

formation of any given particle will be statistically controlled. Naturally, these defects must have a favorable interaction with an embryo of the product phase in order to overcome the nucleation barrier. The very nature of the heterogeneous nucleation suggests that the defects can be induced and, up to a certain thermodynamic limit, eliminated according to the procedure employed to fabricate the  $\text{VO}_2$  samples.

Although a correlation between the size of the precipitates and the characteristic transition temperatures is clear, it is important to consider other possibilities in order to establish a causal linkage. The onset-temperature value of the  $\text{VO}_2$  transition on warming follows the Clapeyron equation.<sup>26</sup> Therefore, an increase in the transition temperature would be expected with an increase in pressure. Using the slope of the Clapeyron equation, the observed increase in the transition temperatures in our samples would imply pressures above 12 GPa, which would be large enough to produce elastic changes in the lattice (see Fig. 7). However, x-ray analysis showed no changes in the lattice constants for any of the different annealing times and sizes investigated. In fact, there is little reason to suspect compressive stress since, at the high implantation doses employed in these experiments, the  $\text{SiO}_2$  substrate is known to relax by plastic flow to accommodate the accumulating stress.<sup>27</sup> The difference between the thermal expansion coefficients cannot explain the effect either, since it has the opposite sign needed to generate a compressive stress on the  $\text{VO}_2$  precipitates. The upper transition temperature is also known to be modified by the presence of dopant impurities—in our case possibly silicon from the substrate. However, silicon doping in bulk samples has no effect. It has been shown that the  $\text{Si}^{4+}$  ion is too small to remain inside the  $\text{VO}_2$  octahedral sites.<sup>3,28</sup> Other doping experiments have shown that the dopant concentration increases with the annealing time. Since the longest annealing times result in the most “bulk-like” nanocrystals, this argues against Si in-



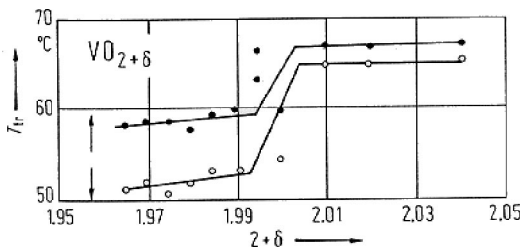


FIG. 8. Transition temperatures vs stoichiometry (taken from Ref. 30). Solid circles: on heating. Open circles: on cooling.

corporation. The other source of possible transition-temperature modification would be departures from the 1:2  $\text{VO}_2$  stoichiometry at short annealing times. These deviations cannot be large; otherwise, vanadium would take other oxide forms with significantly different transition temperatures or there would be no transition at all. Early papers associated the most stoichiometric samples with the largest hysteresis but did not report any change in the upper transition temperature.<sup>29</sup> However, other measurements have shown that the oxygen content is not related to the hysteresis and have proved that small oxygen depletions lower the transitions up to  $8^\circ\text{C}$  while oxygen-rich

samples produced only an increase of up to  $2^\circ\text{C}$ ,<sup>30</sup> as shown in Fig. 8.

#### IV. CONCLUSION

We can conclude that our nanocomposite samples are not showing a stoichiometric or pressure effect, but rather a true size effect. The  $\text{VO}_2$  semiconductor-to-metal phase transition proceeds in a heterogeneous fashion, relying on structural defects as the source of nucleation sites. The size dependence of the transition temperatures and hysteresis loops observed in these small-particle experiments establishes the statistical nature of these activation sites and allows us to obtain experimental values for  $\rho$ . Finally, a power-law function of the driving force has been confirmed as phenomenologically appropriate to describe the density of potent defects.

#### ACKNOWLEDGMENTS

This research was sponsored by the Laboratory Directed Research and Development Program of Oak Ridge National Laboratory, for the U.S. Department of Energy under Contract No. DE-AC05-00OR22725, by the U.S. Department of Energy, Office of Science (Nanoscience, Engineering and Technology program, Grant No. DE-FG02-01ER45916), and by Vanderbilt University's College of Arts and Science.

\*Also at Vanderbilt University, Department of Physics and Astronomy; electronic address: rene.lopez@vanderbilt.edu

†Also at Solid State Division, Oak Ridge National Laboratory.

<sup>1</sup>F.J. Morin, Phys. Rev. Lett. **3**, 34 (1959).

<sup>2</sup>D. Kucharczyk and T. Niklewski, J. Appl. Crystallogr. **12**, 370 (1979).

<sup>3</sup>J.B. Goodenough, J. Solid State Chem. **3**, 490 (1971).

<sup>4</sup>D. Paquet and P. Leroux-Hugon, Phys. Rev. B **22**, 5284 (1980).

<sup>5</sup>M. Gupta, A.J. Freeman, and D.E. Ellis, Phys. Rev. B **16**, 3338 (1977).

<sup>6</sup>R.M. Wentzcovitch, W.W. Schulz, and P.B. Allen, Phys. Rev. Lett. **72**, 3389 (1994).

<sup>7</sup>M. Borek, F. Quian, V. Nagabushnam, and R.K. Singh, Appl. Phys. Lett. **63**, 3288 (1993).

<sup>8</sup>F.C. Case, J. Vac. Sci. Technol. A **2**, 1509 (1984).

<sup>9</sup>J.F. DeNatale, P. Hood, and A.B. Harker, J. Appl. Phys. **66**, 5844 (1989).

<sup>10</sup>F. Guinneton, L. Sauques, J.C. Valmalette, F. Cros, and J.R. Gavarrri, J. Phys. Chem. Solids **62**, 1229 (2001).

<sup>11</sup>F. Guinneton and J.C.V.J.R. Gavarrri, Opt. Mater. **15**, 111 (2000).

<sup>12</sup>R. Lopez, L.A. Boatner, T.E. Haynes, R.F. Haglund, and L.C. Feldman, Appl. Phys. Lett. **79**, 3161 (2001).

<sup>13</sup>S.H. Tolbert and A.P. Alivisatos, Science **256**, 373 (1994).

<sup>14</sup>L.A. Gea and L.A. Boatner, Appl. Phys. Lett. **68**, 3081 (1996).

<sup>15</sup>F. J. Ziegler, *Transport and Range of Ion in Matter*, Version 96.01 (IBM Research, Yorktown Heights, NY, 1996).

<sup>16</sup>C. N. R. Rao and K. J. Rao, *Phase Transitions in Solids* (McGraw-Hill, New York, 1978).

<sup>17</sup>Without additional stress terms that would enhance the energy requirements for the transition.

<sup>18</sup>C.N. Berglund and H.J. Guggenheim, Phys. Rev. **185**, 1022

(1969).

<sup>19</sup>G.B. Stainchowiak and P.G. McCormick, Acta Metall. **36**, 291 (1988).

<sup>20</sup>A. Cavalleri, C. Tóth, C.W. Siders, J.A. Squier, F. Ráksi, P. Forget, and J.C. Kieffer, Phys. Rev. Lett. **87**, 237401 (2001).

<sup>21</sup>J. E. Freund and R. E. Walpole, *Mathematical Statistics* (Prentice-Hall, Englewoods Cliffs, NJ, 1987).

<sup>22</sup>If defects appear at particle surfaces,  $V$  is replaced by  $V^{2/3}$  in the exponential function. However, our  $\text{VO}_2$  precipitates are large enough to make the ratio of surface atoms to volume atoms quite small and they, in fact, show a better fit to the model using volumetric defects.

<sup>23</sup>L.-W. Chen, Y.-H. Chiao, and K. Tsukazi, Acta Metall. **33**, 1847 (1985).

<sup>24</sup>Given their extrinsic nature, we do not expect their activation to follow a Boltzman distribution.

<sup>25</sup>This asymmetric shear stress is probably the energy barrier responsible for the large undercooling and it is assumed to be a standard feature of a good-quality  $\text{VO}_2$  crystal. It should not be confused with matrix stress, which seems to be ruled out by the data shown in Fig. 7.

<sup>26</sup>C.N. Berglund and A. Jayarama, Phys. Rev. **185**, 1034 (1969).

<sup>27</sup>F. Harbsmeier, J. Conrad, and W. Bolse, Nucl. Instrum. Methods Phys. Res. B **136**, 505 (1998).

<sup>28</sup>J.B. MacChesney and H.J. Guggenheim, J. Phys. Chem. Solids **30**, 225 (1969).

<sup>29</sup>K. Kimizuka, M. Ishii, I. Kawada, M. Saeki, and M. Nakahira, J. Solid State Chem. **9**, 69 (1974).

<sup>30</sup>C. Blauw, F. Leenhouts, F.V. der Woude, and G.A. Sawatzky, J. Phys. C **8**, 459 (1975).